

Lower-hybrid breakdown of gas in the field of a current-carrying loop in a plasma-filled magnetic confinement system

G. Yu Golubyatnikov, S. V. Egorov, B. G. Eremin, A. G. Litvak, A. V. Strikovskii, O. N. Tolkacheva, and Yu. V. Chugunov

Institute of Applied Physics, Russian Academy of Sciences 603600, Nizhniĭ, Novgorod, Russia
(Submitted 22 August 1994)

Zh. Eksp. Teor. Fiz. **107**, 441–449 (February 1995)

Experiments have been carried out on the breakdown dynamics and the formation of an ionized region in the field of a current-carrying loop in a large magnetic confinement system filled with background plasma. The loop radiates in the lower-hybrid frequency range. Breakdown is observed to generate a strong local perturbation of plasma: $\Delta N/N \approx 10^2$, $\Delta T_e/T_e \approx 50$. The perturbed region has a transverse dimension roughly equal to the antenna diameter. Along the direction of the magnetic field, this region is localized between the magnetic mirrors. The density begins to increase throughout the volume of this magnetic tube at the instant at which the field arises at the antenna. Analysis of experimental data leads to the conclusion that the primary cause of the fast ionization along the magnetic force tube is the excitation of an intense beam of lower-hybrid plasma waves. © 1995 American Institute of Physics.

1. INTRODUCTION

The problem of efficiently depositing electromagnetic energy in a plasma is of much importance to the efforts to achieve rf heating, to excite intense plasma turbulence, and to perturb geophysical processes in the earth's ionosphere and magnetosphere in order to study plasma-wave phenomena and wave-particle interactions. Of particular interest in the problem of artificially altering the parameters of the ionospheric and magnetospheric plasma is the development and refinement of methods for "active" plasma diagnostics.

Experiments which have been carried out^{1–6} in space and in the laboratory have shown that electromagnetic waves generated in the rf range by an on-board dipole antenna can be a method for generating strong perturbations of the plasma and for stimulating precipitation of high-energy electrons and ions. Laboratory experiments^{7,8} have demonstrated local heating and the formation of controllable plasma formations can be achieved in a magnetized plasma in the field of a dipole antenna radiating in the lower-hybrid frequency range. In the present paper we are reporting a study of lower-hybrid breakdown in the field of a current-carrying loop. This study was carried out in a large magnetic confinement system filled with a background plasma. Our major goal in this study was to learn about the spatial dynamics of the plasma formations generated in the field of the current-carrying loop.

2. DESCRIPTION OF THE EXPERIMENTAL APPARATUS

The experiments were carried out in a mirror magnetic confinement system in a vacuum chamber 10 m long and 3 m in diameter (Fig. 1). The length of the magnetic confinement system was $L = 3.5$ m, its diameter was $D = 1.5$ m, its mirror ratio was $\sigma = 2$, and the maximum magnetic field at the mirrors was $B_{0 \max} = 750$ G. A background plasma was produced in the system by creating an induction discharge in argon at a pressure $P = 5 \times 10^{-5}$ torr. In an effort to achieve a fairly uniform longitudinal distribution of the background

plasma, we placed six inductors in a uniform arrangement in several cross sections of the confinement system. These inductors, 1.2 m in diameter, were connected to three rf oscillators, each with an output power $P = 1$ MW.

All the measurements were carried out with decaying quasisteady background plasma (the typical decay time was $\tau_N = 1.5$ ms) at electron and ion temperatures $T_{e,i0} = 0.5$ eV. The radial profile of the plasma density was approximately parabolic: $N_0 = N_{0\max}(1 - \beta^2 r^2)$, where $N_{0\max} = 4 \times 10^{11}$ cm⁻³, $\beta^{-1} = 0.6$ m, and r is the distance from the axis of the confinement system. A perturbed region was created in the background plasma by arranging the breakdown of gas injected into the plane of the loop, which was at one of the magnetic mirrors, near the surface of the lower-hybrid resonance $\omega \geq \Omega_{LH} = (\omega_{Be}\omega_{Bi})^{1/2}$, $\omega_{pe} \geq \omega_{Be}$ (ω_{pe} is the electron plasma frequency, ω_{Be} is the electron cyclotron frequency, and ω_{Bi} is the ion cyclotron frequency). The loop had a radius $a = 9$ cm. The plane of the loop was oriented perpendicular to the magnetic field lines. The power fed to the antenna was $P_A \approx 0.5$ MW at the frequency $f = 5$ MHz. The rf current pulse length was either $\tau_A = 100$ or 600 μ s. The amplitude of the current in the antenna was $I_A \approx 100$ A. In this case the electron oscillation energy ϵ_{\sim} in the vicinity of the loop was on the order of the ionization potential of the gas, $I_i^{Ar} = 15.8$ eV.

In experiments, the gas was injected by means of a controlled vacuum valve which made it possible to turn on the antenna at various values of the pressure ($\Delta P = 10^{-4}$ – 10^{-2} torr), with various distributions of the gas density. Figure 2 shows curves of the time evolution (of the gas pressure ΔP , of the magnetic field B_0 , and of the rf voltage pulses) to characterize the operating conditions of the apparatus. Also shown in this figure is the typical distribution of the gas pressure in the system, which was measured with a movable PMI-10 gauge. The charged-particle density was measured by a six-channel microwave interferometer at the wavelength $\lambda_0 = 8$ mm and by microwave-resonance probes. In studying the heating of the plasma electrons we used symmetric

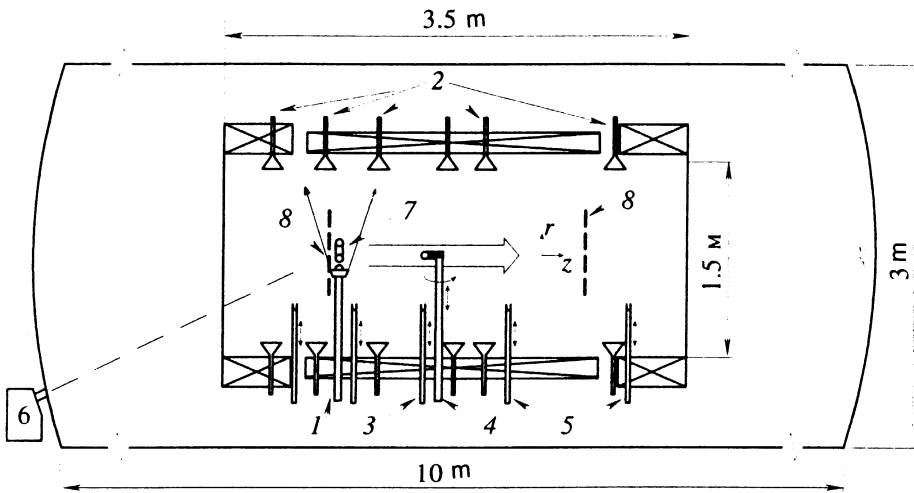


FIG. 1. Experimental layout and arrangement of the diagnostic apparatus. 1—Gas injector; 2—multichannel microwave interferometer; 3—microwave-resonance probe; 4—multigrid probe; 5—double probes; 6—multichannel electron-energy analyzer; 7—antenna; 8—geometric arrangement of the cross sections of the lower-hybrid resonance, with $\omega = \Omega_{LH}$; Here $P_0 = 8 \times 10^{-6}$ torr.

probes positioned along the radius in several cross sections of the confinement system. The joint measurements by the interferometric and probe methods, along with the good reproducibility of the plasma parameters in each working cycle of the apparatus, made it possible to study the space-time evolution of the perturbed region. Energy spectra of the accelerated charged particles generated in the confinement system as a result of the rf breakdown were measured by a multigrid probe, which was moved by varying its radial position and angle θ .

3. EXPERIMENTAL RESULTS AND DISCUSSION

When the pulse of rf current flows through the loop, we observe a pronounced increase in the plasma density and temperature in the vicinity of the loop. The rise time of the discharge and the maximum values of the density and temperature of the charged particles depend strongly on the density of injected gas. Figure 3 shows the time evolution of the plasma density, $\Delta N(t)$, measured at various distances from the loop by the multichannel interferometer. In analyzing the

interferograms we allowed for the time evolution of the transverse profile of the perturbed region and of its size.

Tables I and II show the basic relations and parameters of the plasma in the background region (a) and in the perturbed region (b). It can be seen from Table II that the charged-particle density near the antenna, under the conditions $\Delta P \approx 10^{-2}$ torr and $\tau_A = 690 \mu s$, rises by more than two orders of magnitude, while the electron temperature rises by a factor of 30. At pressure $\Delta P \approx 10^{-4}$ torr the density increases by an order of magnitude, but the temperature rises by a factor of 60. Estimates show that in the first case the relations $\nu_e^{eff}/\omega \gg 1$ and $l_e^{eff} \ll a$, hold, while in the second the relations $\nu_e^{eff}/\omega \ll 1$ and $l_e^{eff} \gg a$, hold, where ν_e^{eff} and l_e^{eff} are the effective collision rate and mean free path of the electrons in the perturbed region.

It follows from the probe measurements that the perturbed region in the direction perpendicular to \mathbf{B}_0 is smaller than the antenna diameter during the operation of the source and that this size decreases slightly with distance from the antenna. Figure 4 shows some typical radial profiles of the

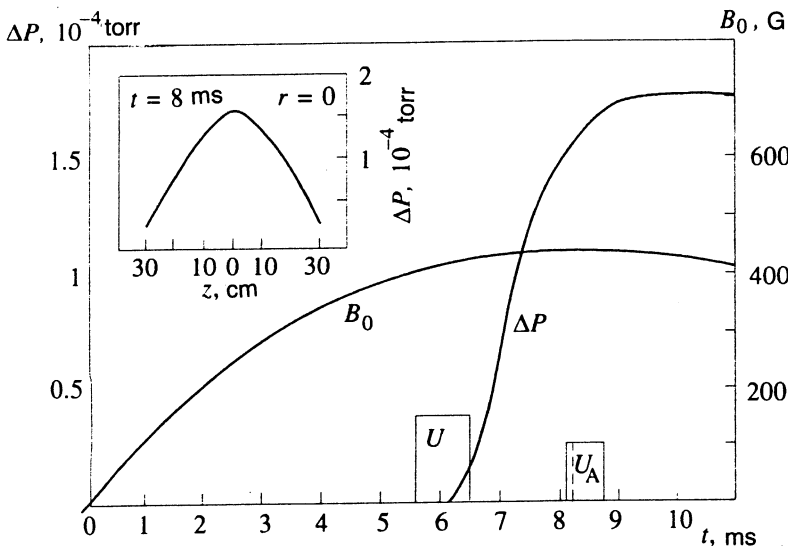


FIG. 2. Operating conditions of the apparatus. Shown here is the time evolution of the magnetic-field amplitude B_0 and of the injected-gas pressure ΔP near the source, of the amplitude of the rf voltage at the inductors, U , and of that at the antenna, U_A . The inset at the upper left shows the profile of the pressure of neutral particles along the axis of the system.

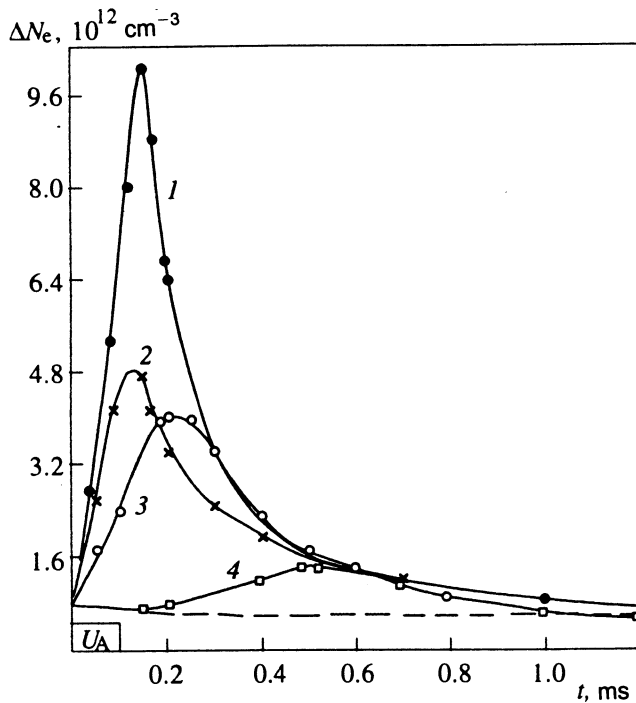


FIG. 3. Time evolution of the charged-particle density in the perturbed region of the plasma at various distances from the source ($\tau_A = 100 \mu\text{s}$, $\Delta P = 1.5 \times 10^{-4}$ torr). 1— $z = 23$ cm; 2—75; 3—105; 4—185 cm. The dashed line shows the background-plasma density.

current density as measured by a double probe operating under saturation ion-current conditions, $I_{oi} \sim N \sqrt{T_e}$, at a distance of 125 cm (along the axis of this system) at the time $t = 560 \mu\text{s}$ (with $\tau_A = 100 \mu\text{s}$). The longitudinal dimension of the perturbed region during the operation of the source depends on both the length of the rf current pulse in the antenna and the pressure of injected gas, ΔP , but it is less than the distance between magnetic mirrors (Fig. 5, a and b).

Turning to the dynamics of the breakdown, we focus on the case of primary interest (from the standpoint of active experiments in the ionospheric plasma): that in which the conditions $\nu_e^{\text{eff}}/\omega \ll 1$ and $l_e^{\text{eff}} \gg a$ hold in the perturbed region of the plasma. It follows from the experimental data that in the initial stage of the breakdown a fast ionization mechanism operates along the magnetic force tube. The charged-particle density begins to rise at the time at which the field is turned on at the source, both in the vicinity of the source and at fairly large distances away from it ($l > 100$ cm; Fig. 3). In the cross section $l = 185$ cm, however, which is beyond the lower-hybrid-resonance plane, the density begins to increase at a time $\Delta t \approx 150 \mu\text{s}$ after the beginning of generation.

It can be concluded from these results that one possible mechanism for the development of the discharge involves

TABLE I. Parameters of the background plasma.

P , torr	N_a , cm^{-3}	N_e , cm^{-3}	$T_e = T_i$, eV	ν_{ei} , s^{-1}	l_e , cm	ν_{ia} , s^{-1}	$B_0(z = z_A)$, G
$5 \cdot 10^{-3}$	$2 \cdot 10^{12}$	$2 \cdot 10^{11}$	0.5	$2.3 \cdot 10^7$	2	$2.3 \cdot 10^{-3}$	440

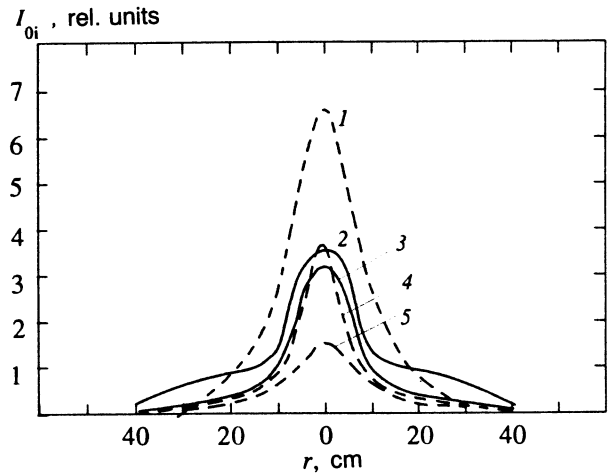


FIG. 4. Radial profiles of the saturation ion current $I_{oi} \sim N \sqrt{T_e}$ at various times during the flow of the rf current in the antenna, at a distance $z = 125$ cm from the antenna ($\tau_A = 100 \mu\text{s}$, $\Delta P = 1.5 \times 10^{-4}$ torr). 1— $t = 170 \mu\text{s}$; 2—100; 3—60; 4—520 5—920 μs .

additional ionization in the electric field of plasma waves excited by the current-carrying loop. Specifically, because of the dispersion properties of the plasma in the lower-hybrid frequency range for the given source geometry [the dimensions of the current-carrying loop are $a \ll \lambda_{EM}$, where $\lambda_{EM} \approx \sqrt{2\pi(c/\omega)(\omega_{Be}/\omega_{pe})}$ is the wavelength of an electromagnetic mode], an intense beam of plasma waves is generated. This beam propagates at a small angle from the magnetic field, $\alpha \approx \omega/\omega_{Be}$, where α is the angle between the group velocity and the magnetic field. In the experiments the relation $\omega/\omega_{Be} \ll 1$ held. It follows from estimates⁹ that the electric-field amplitude of the plasma waves at a distance $l = 2$ m is $E_r \approx \sqrt{2(\omega\omega_{pe}/c^3)(\sqrt{\omega/\omega_{Be}})aI_A} \approx 10$ V/cm and is considerably higher than the amplitude of the breakdown field, $E_{br} \approx \omega/e\sqrt{2I/m_e} \approx 4$ V/cm. As a result, ionization can occur quite rapidly at large distances from the antenna (at distances several times the value of λ_{EM} ; Refs.9 and 10). At the same time, the lower-hybrid-resonance surfaces are reflecting surfaces at the magnetic mirrors, beyond which the waves in this part of the spatial spectrum (resonant plasma waves) do not penetrate. In this geometry we are essentially dealing with a quasioptical resonator for lower-hybrid plasma waves. In the initial stage of the breakdown, the background plasma is the slow-wave system. Later on, as nonlinear ionization process develop, this role is played by the self-consistent three-dimensional plasma irregularity, which approaches a steady state (in terms of the values of the temperature and density of the charged particles) in the case of long pump pulses.

Another possible cause of the fast ionization might be

TABLE II. Parameters of the plasma in the perturbed region.

τ_A , μs	ΔP , torr	$\langle \Delta T_e \rangle$, eV	$\langle \Delta N \rangle$, cm^{-3}	ΔN_{max} , cm^{-3}	ν_e^{eff} , s^{-1}	ν_e/ω	l_e , cm	ν_{ia} , s^{-1}	ν_e/ω_{Be}	ν_{ia}/ω_{Bi}	L_{\parallel} , cm
600	$1.5 \cdot 10^{-4}$	30	$4 \cdot 10^{12}$	$8 \cdot 10^{12}$	$2.8 \cdot 10^6$	$\ll 1$	$1.2 \cdot 10^2$	$5 \cdot 10^3$	$4 \cdot 10^{-4}$	$5.4 \cdot 10^{-2}$	200
	$1.5 \cdot 10^{-3}$	20	10^{13}	$2 \cdot 10^{13}$	$2.6 \cdot 10^7$	~ 1	10	$4.3 \cdot 10^4$	$3.7 \cdot 10^{-3}$	0.5	70
	$1.5 \cdot 10^{-2}$	14	$2 \cdot 10^{13}$	$> 2 \cdot 10^{13}$	$2.4 \cdot 10^8$	$\gg 1$	1	$4.5 \cdot 10^5$	$3.4 \cdot 10^{-2}$	5	40
100	$1.5 \cdot 10^{-4}$	4.5	$4 \cdot 10^{12}$	$9 \cdot 10^{12}$	$9 \cdot 10^6$	< 1	14	$5 \cdot 10^3$	$1.3 \cdot 10^{-3}$	$5 \cdot 10^{-2}$	80
	$5 \cdot 10^{-3}$	2	$6 \cdot 10^{12}$	$\gtrsim 10^{13}$	$1.3 \cdot 10^8$	> 1	0.7	$2.3 \cdot 10^5$	$2 \cdot 10^{-2}$	2.5	50

electrons which are accelerated directly in the induction zone and for which the ionization length is $l_i > 100$ cm. The measurements taken with the multigrid probe showed that intense fluxes of accelerated electrons with energies up to and exceeding 100 eV are generated parallel to \mathbf{B}_0 . Such electrons are also capable of causing additional ionization of the background plasma at a large distance ($l > 100$ cm) from the source.

The spatial dynamics of the development of the breakdown in the presence of a background plasma is apparently affected by both the plasma-wave mechanism and the accelerated electrons generated near the source.

The further increase in the charged-particle density and the filling of the magnetic force tube by these particles result primarily from two processes: ionization of the injected gas cloud and quasineutral motion of plasma out of this region. At $\tau_A = 100 \mu\text{s}$ the maximum density N_{max} is reached after the rf current in the antenna is turned off. This effect can occur at fairly high values of the energy deposition in the plasma, at which the average thermal energy of the particles has become comparable in magnitude to, or greater than, the ionization energy of the atoms by the time at which the source is turned off. A sufficient condition here is that the rate of gas ionization (caused by the fast electrons present in the plasma) after the field at the source is turned off be higher than the rate at which charged particles are lost. In this case the losses are determined primarily by the displacement of the particles by diffusion or by quasineutral dispersal (depending on the relation between the electron mean free path l_e and the length scale of the irregularity of the ionized region, L_{\parallel}) along \mathbf{B}_0 . The time scale of the electron cooling which results from collisions with heavy particles is $\tau_{T_e} = (\delta \nu_e^{\text{eff}})^{-1} \approx 4$ ms in the perturbed region ($\delta = 2m_e/M_i$, where M_i is the mass of an ion), and the time scale of the recombination losses is $\tau_r \approx 1$ s.

The relaxation of the ionized region after the rf source is turned off depends strongly on the duration of the current pulse in the antenna. At $\tau_A = 100 \mu\text{s}$, for example, the parameters of the ionized region are such that the condition $l_e/L_{\parallel} \ll 1$ holds, and we observe diffusive decay of the plasma. An estimate of the time scale of the ambipolar diffusion of charged particles along the magnetic field, $\tau_{N_{\parallel}} \approx L_{\parallel}^2 \nu_{ia}/v_s^2$, yields $140 \mu\text{s}$ (here $\nu_{ia} \approx 5 \times 10^3 \text{ s}^{-1}$ is the rate at which ions collide with neutrals, which is determined by resonant charge exchange; $v_s \approx 5 \times 10^5 \text{ cm/s}$ is the ion acoustic velocity; and $L_{\parallel} \approx 80$ cm). This figure agrees fairly well with the measured value of $\tau_N \approx$ near the antenna (at $l \approx 25$ cm). Far from the source ($l > 100$ cm) the decay time

increases, reaching $\tau_N \approx 300 \mu\text{s}$. The apparent reason for this result is the effect of the magnetic mirrors on the diffusion of the charged particles. When the length of the current pulse in the antenna is $\tau_A = 600 \mu\text{s}$, the relaxation of the plasma density begins slightly before (at $t \approx 400 \mu\text{s}$) the source is turned off. At this time, the losses of charged particles from the ionized region due to quasineutral dispersal have evidently become substantial, by virtue of the relation $l_e > L_N$. There is initially a rapid decay of the density ($\tau_N \leq 300 \mu\text{s}$), and then the relaxation slows down. As a result of the (now) diffusive decay, the perturbed region relaxes to the background level.

On the whole, the spatial dynamics of the decay of the perturbed region is quite complex, depending on the duration of the pump field, the pressure of injected gas, and the parameters of the ionized region. We should point out that the plasma relaxation is accompanied by precipitation of charged particles from the magnetic confinement system. In the experiments, these precipitated particles were detected by a multichannel electrostatic energy analyzer at a distance $L = 2$ m from the solenoid.

4. CONCLUSION

These experiments have thus demonstrated that this method for depositing energy in a given volume of a magnetic force tube is efficient and that the deposition can be controlled by varying the parameters of the source, e.g., ΔP and τ_A . For example, the typical efficiency of the energy deposition for a source with $\Delta P = 10^{-4}$ torr and $\tau_A = 100 \mu\text{s}$ is $\eta = P_{\text{abs}}/P_A \approx (\langle \Delta N \rangle \langle \Delta T \rangle) V \tau_A^{-1} / P_A \approx 0.2$ [here $\langle \Delta N \rangle$ and $\langle \Delta T \rangle$ are the mean values of the electron density and temperature in the volume (V) occupied by the discharge plasma]. Accordingly, sources of this type look promising for experiments in space, particularly in the upper layers of the earth's ionosphere, where dipole sources of radiation in the whistler frequency range are inefficient because of the small ratio of the wavelength of the electromagnetic wave to the size of the antenna and also because of the relatively low charged-particle density. Drawing a comprehensive picture of lower-hybrid breakdown in a plasma-filled magnetic confinement system will of course require, in addition to a detailed theoretical analysis, a detailed study of the dynamics and structure of the electromagnetic field of the source, a study of its input characteristics, and a study of the energy distribution of the charged particles and of the spectra of noise radiation during the development of the discharge and after the discharge is turned off.

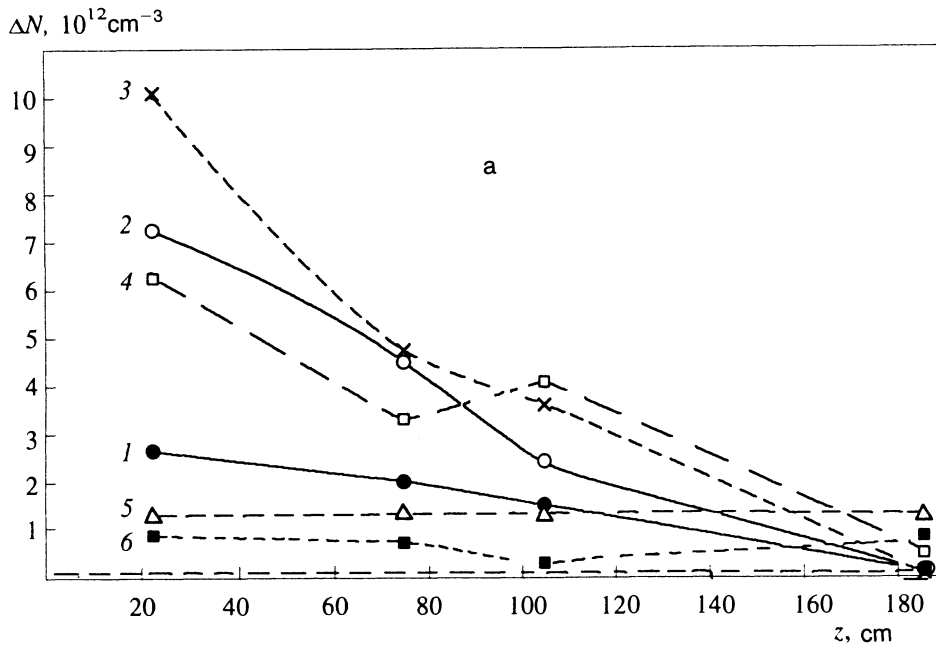
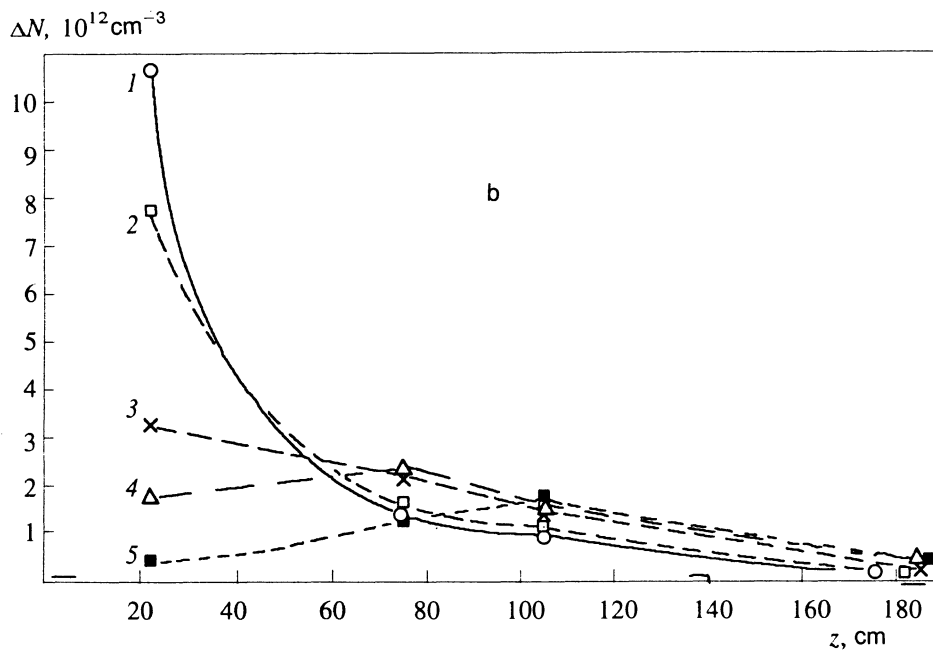


FIG. 5. Longitudinal profiles of the charged-particle density in the perturbed region of the plasma at various times. a: $\tau_A = 100 \mu\text{s}$, $\Delta P \approx 1.5 \times 10^{-4}$ torr. 1— $t = 40 \mu\text{s}$; 2—100; 3—150; 4—200; 5—600; 6—1000 μs . The dashed line at the bottom shows the background-plasma density. b: $\tau_A, \Delta P \approx 5 \times 10^{-3}$ torr. 1— $t = 100 \mu\text{s}$; 2—200; 3—400; 4—600; 5—1000 μs .



Finally, we note that the experimental data obtained in the present study may prove useful for planning active experiments in space. In terms of scaling properties ($\omega_{pe} \gg \omega_{Be} \gg \nu_{ei} \gg \nu_{ea}, M_i \nu_{ia} \gg m_e \nu_e$) the laboratory plasma corresponds to the plasma in the upper layers of the earth's ionosphere. The particular ionization source was chosen in an effort to keep the refractive index ($n = c/f\lambda_{EM}$) for the radiated electromagnetic waves with frequencies in the range $\Omega_{LH} \leq 2\pi f \leq \omega_{Be} \leq \omega_{pe}$ in the magnetized plasma at a value such that the inequalities $a \ll \lambda_{EM} \ll L$ were satisfied. Such high values of the energy supplied to the source were dictated by the desire to maintain a value $E/E_{br} \approx (E/\omega)e/\sqrt{2I_i m_e} \propto E/\omega$ ($I_i^{air} \approx 15$ eV, $I_i^{Ar} \approx 15.8$ eV) under laboratory and ionospheric conditions.

This study was supported by the Russian Fund for Fundamental Research (Grant No. 93-02-848).

- ¹ Yu. I. Gal'perin, R. Z. Sagdeev, F. K. Shuiskaya *et al.*, *Kosm. Issled.* **19**, 34 (1981)
- ² Yu. N. Agafonov, V. S. Bazhanov, Yu. I. Gal'perin *et al.*, *JETP Lett.* **52**, 530 (1990).
- ³ Yu. N. Agafonov, V. S. Bazhanov, Yu. I. Gal'perin *et al.*, *Pis'ma Zh. Tekh. Fiz.* **16**(16), 65 (1990) [*Sov. Tech. Phys. Lett.* **16**, 627 (1990)].
- ⁴ G. Yu. Golubyatnikov, S. V. Egorov, A. V. Kostrov *et al.*, *Zh. Eksp. Teor. Fiz.* **96**, 2009 (1989) [*Sov. Phys. JETP* **69**, 1134 (1989)].
- ⁵ R. L. Stenzel and W. Geckelman, *Phys. Fluids* **20**, 108 (1977).
- ⁶ H. Sugai, M. Maruyama, M. Sato, and S. Takeda, *Phys. Fluids* **24**, 690 (1978).
- ⁷ G. Yu. Golubyatnikov, S. V. Egorov, A. V. Kostrov *et al.*, *Fiz. Plazmy* **14**, 482 (1988) [*Sov. J. Plasma Phys.* **14**, 285 (1988)].

⁸S. V. Egorov, A. V. Kostrov, and A. V. Tronin, Zh. Eksp. Teor. Fiz. **94**(4), 124 (1988) [Sov. Phys. JETP **67**(4), 717 (1988)].

⁹G. Yu. Golubyatnikov, S. V. Egorov, A. V. Kostrov *et al.*, Zh. Eksp. Teor. Fiz. **94**, 124 (1988) [Sov. Phys. JETP **67**, 717 (1988)].

¹⁰E. A. Mareev and Yu. V. Chugunov, *Antennas in Plasmas* [in Russian] (IFP Russ. Akad. Nauk, Nizhniĭ Novgorod, 1991).

Translated by D. Parsons